

Original Article

TAGLN expression decreases in the wall of unruptured intracranial aneurysms in Chinese population

Xue Xia, Tianyu Shao, Jing Luo, Xing Zhang, Mingyue Bao, Lei Ye, Hongwei Cheng

Department of Neurosurgery, The First Affiliated Hospital of Anhui Medical University, Jixi 218, Hefei 230022, P. R. China

Received November 26, 2019; Accepted March 3, 2020; Epub May 15, 2020; Published May 30, 2020

Abstract: Background: The rupture of intracranial aneurysm (IA) is the primary cause of subarachnoid hemorrhage with high mortality and morbidity. However, there were no effective treatment options prior to the rupture of IA, except for surgical treatment or endovascular therapy, which might lead to complications. Therefore, biomolecule-based therapeutic model should be investigated. Methods: A total of 5 selected GEO datasets were chosen. Protein-protein interaction was conducted with the STRING and MCODE plug-in tool. Gene ontology analysis and KEGG pathway enrichment were also conducted using the DAVID database. Real-time PCR was applied for analyzing the differential expressions of TAGLN and TPM1 among 16 unruptured vessels and 10 normal superficial temporal arteries. Results: We found no common DEGs, biological processes, molecule functions and KEGG pathway enrichments among the selected GEO datasets. Total of 102 common DEGs were found between GSE26969 and GSE46337, which were two Chinese population-based datasets. Module analysis showed that IA was correlated with vascular smooth muscle contraction related genes and major histocompatibility complex (MHC) gene cluster related genes. The expression of TAGLN was replicated to be decreased in the unruptured IA vessels ($P = 0.003$). Conclusion: This bioinformatic analysis demonstrated the correlations between IA and MHC gene cluster as well as vascular smooth muscle contraction related genes. TAGLN was initially replicated to be decreased in the unruptured vessels of IA patients. It might provide potential biomolecules for therapeutic target of IA.

Keywords: Intracranial aneurysm, major histocompatibility complex, vascular smooth muscle

Introduction

Intracranial aneurysm (IA), also termed cerebral aneurysm, is a potentially devastating cerebrovascular disorder characterized by ballooning or localized abnormal widening of a cerebral artery lumen or arterial wall [1]. The global prevalence of IA is approximately 3.2% [2]. Most IA does not rupture and remains asymptomatic during a person's life. However, it was also reported that after IA ruptured, it caused subarachnoid hemorrhage (SAH) with the notably high mortality and severe sequelae [3, 4]. Despite the considerable progresses of modern therapeutic technology, there is still a lack of preventive treatments prior to the occurrence of IA rupture. Meanwhile, complications and less favorable long-term outcomes are observed due to the invasive procedures of surgical treatment and endovascular therapy [5]. Therefore, screening novel biomarkers that

might potentially be applied as molecular therapeutic models may help to cure IA or prevent IA from rupturing.

In recent decades, high-throughput screening technologies for biomolecules, including genes, RNAs and proteins, have been widely applied by researchers. Gene microarray analysis is a potent technique to depict the gene-expression profiles of certain diseases or characteristics. In previous studies, numerous candidate genes or pathway enrichments have been found to be associated with the risk of IA according to the gene-expression screening methods [6, 7]. However, we found diverse or even discrepant results among these studies. Li et al. found that decreased expression genes of IA were enriched in the immune/inflammation response [8], while Pera et al. found that the genes enriched in that biological process exhibited decreased expression in IA patients [9]. Meanwhile, other

Bioinformatic analysis of IA

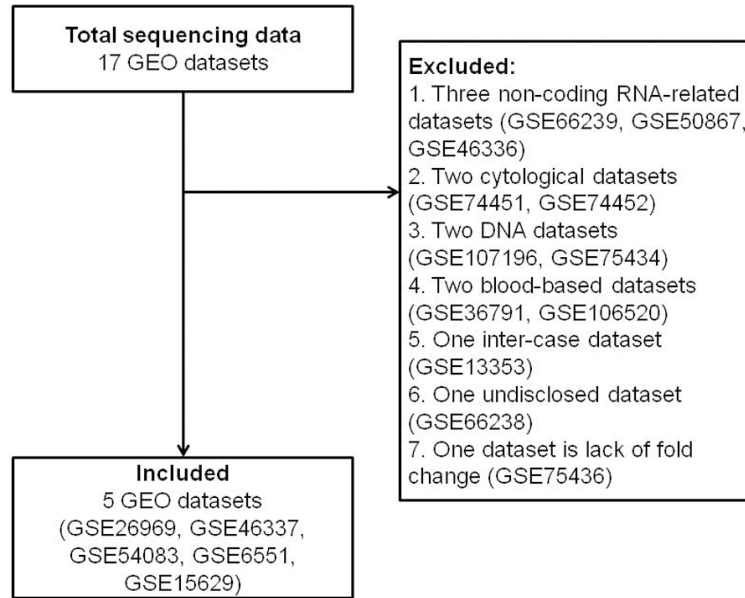


Figure 1. Inclusion and exclusion of GEO datasets.

IA-related biological processes or pathway enrichments were found among studies, such as cell adhesion, muscle system, chemotaxis, and RNA splicing/processing [9-11].

In this study, we compared the differentially expressed genes (DEGs) from several published Gene Expression Omnibus (GEO) datasets of IA-related studies and investigated whether there were common points by using bioinformatic analysis. Meanwhile, protein-protein interaction (PPI), biological process, molecular function, cellular component and Kyoto Encyclopedia of Genes and Genomes (KEGG) pathway enrichment of common DEGs from two Chinese ethnicity-based studies were performed, aiming at visualizing specific relationships among genes and providing potential molecule-based therapeutic targets for Chinese IA patients.

Materials and methods

Patients

A total of 16 unruptured IA tissues and 10 superficial temporal arteries were collected. Informed consent was obtained from all participants included in the study. This study was approved by the Clinical Research Ethics Committee of Anhui Medical University of China. All procedures performed in the study

involving human participants were in accordance with the ethical standards of the institutional and/or national research committee and with the 1964 Declaration of Helsinki and its later amendments or comparable ethical standards.

Research protocols and microarray data

A total of 17 IA-related sequencing datasets from the GEO database were collected. After limited scopes with publicity, free availability and common RNA expression for the dataset (**Figure 1**), five GEO datasets for IA, GSE6551, GSE15629, GSE26969, GSE46337 and GSE54083 were selected for further analysis.

Detailed information, including platforms, sample numbers and ethnicities, is listed in [Supplementary Table 1](#).

Data processing of DEGs

In this study, we re-analyzed the results from each dataset in a standard software, GEO2R (<http://www.ncbi.nlm.nih.gov/geo/geo2r/>), which is used for the selection of DEGs between the IA tissues and the normal blood vessels for each GEO dataset with gene symbols. Then the results were put together and the statistics re-done. We simultaneously defined two parameters, that is, adjusted p value < 0.05 and $|\log_{2}FC| > 2$, as the cut-off criteria.

Gene ontology (GO) and KEGG pathway analysis of DEGs

The Database for Annotation, Visualization and Integrated Discovery (DAVID, <http://david.ncifcrf.gov/>), an online bioinformatics resource, was applied for functional interpretation of large lists of genes or proteins. Among these tools, GO was used for annotating genes and gene production in different aspects, including biological processes (BP), molecular function (MF) and cellular component (CC). Additionally, KEGG pathway analysis was another tool employed for interpreting genomes, biological pathways, diseases and chemical substances.

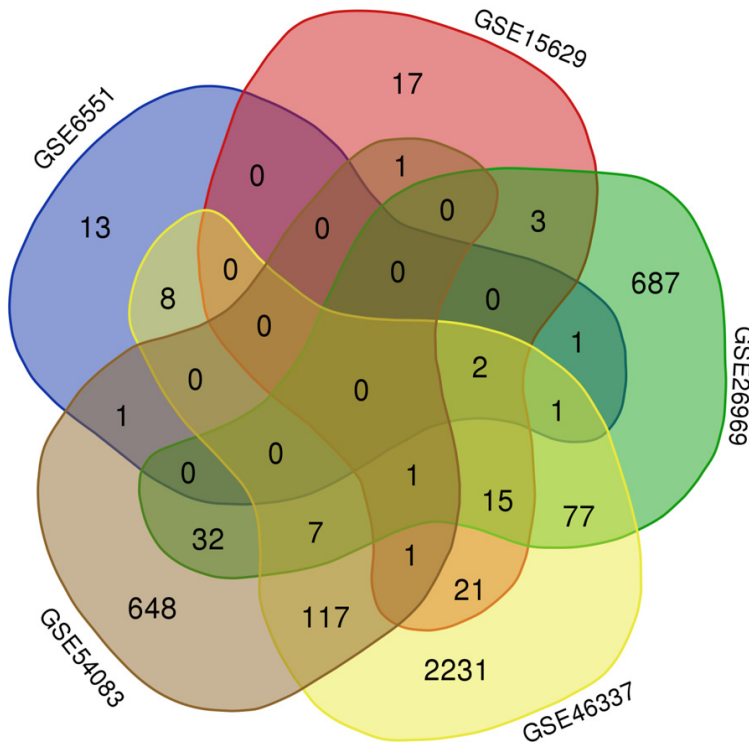


Figure 2. Venn diagram of common differentially expressed genes among the 5 datasets.

PPI network and module analysis

Protein-protein interaction (PPI) information was introduced here to detect potential relationships among DEGs. The Search Tool for the Retrieval of Interacting Gene (STRING) app was applied in Cytoscape with cut-off criteria of confidence score ≥ 0.4 and maximum number of interactors = 0. Meanwhile, the Molecular Complex Detection (MCODE) app was also utilized to screen key modules of the PPI network in Cytoscape with degree cut-off = 2, node score cut-off = 0.2, k-core = 2 and max. depth = 100.

Real-time quantitative PCR on the expression of TPM1 and TAGLN

Total mRNA extracted from vessels using TRIzol (Invitrogen) was reversely transcribed into cDNA (Life Technology). The primers for TPM1, TAGLN and GAPDH were commercially obtained from OriGene Technologies (Rockville, USA), and the information is shown in [Supplementary Table 2](#). Samples were amplified in the Applied Biosystems 7900 HT Fast Real-time PCR system (California, USA). The fold changes of

mRNA expression between TPM1 and TAGLN were compared by $2^{-\Delta\Delta Ct}$.

Statistical analysis

The raw data of each GEO dataset were re-analyzed in an online standard software, GEO2R (<http://www.ncbi.nlm.nih.gov/geo/geo2r/>) which was basically calculated with R script. DEGs between the IA tissues and the normal blood vessels were calculated. Genes with the most significant *P* values will be the most reliable. Moderated F-statistic combines the t-statistics for all the pairwise comparisons into an overall test of significance for that gene.

SPSS software (Version 19.0, SPSS Inc, Chicago, IL, USA) was applied for statistical analysis. All enumeration data were analyzed with a nonparametric t test. The *p*-values reported in the study were based on a two-sided probability test with a significance level of $P < 0.05$.

Results

Identification of DEGs

Based on the GEO2R online analytic tool, with the criteria of adjusted $P < 0.05$ and $|\log_2FC| > 2$, we calculated DEGs for each GEO dataset. Generally, a total of 25 DEGs were detected for GSE6551, of which 18 genes were up-regulated and 7 genes were down-regulated. A total of 60 DEGs were detected for GSE15629, of which 21 genes were up-regulated and 39 genes were down-regulated. A total of 825 DEGs were detected for GSE26969, of which 814 genes were up-regulated and 11 genes were down-regulated. A total of 2834 DEGs were detected for GSE46337, of which 1345 genes were up-regulated and 1489 genes were down-regulated. Finally, a total of 822 DEGs were detected for GSE54083, of which 470 genes were up-regulated and 352 genes were down-regulated. Meanwhile, we found no common DEGs after we compared all the DEGs from the 5 datasets (**Figure 2**).

Bioinformatic analysis of IA

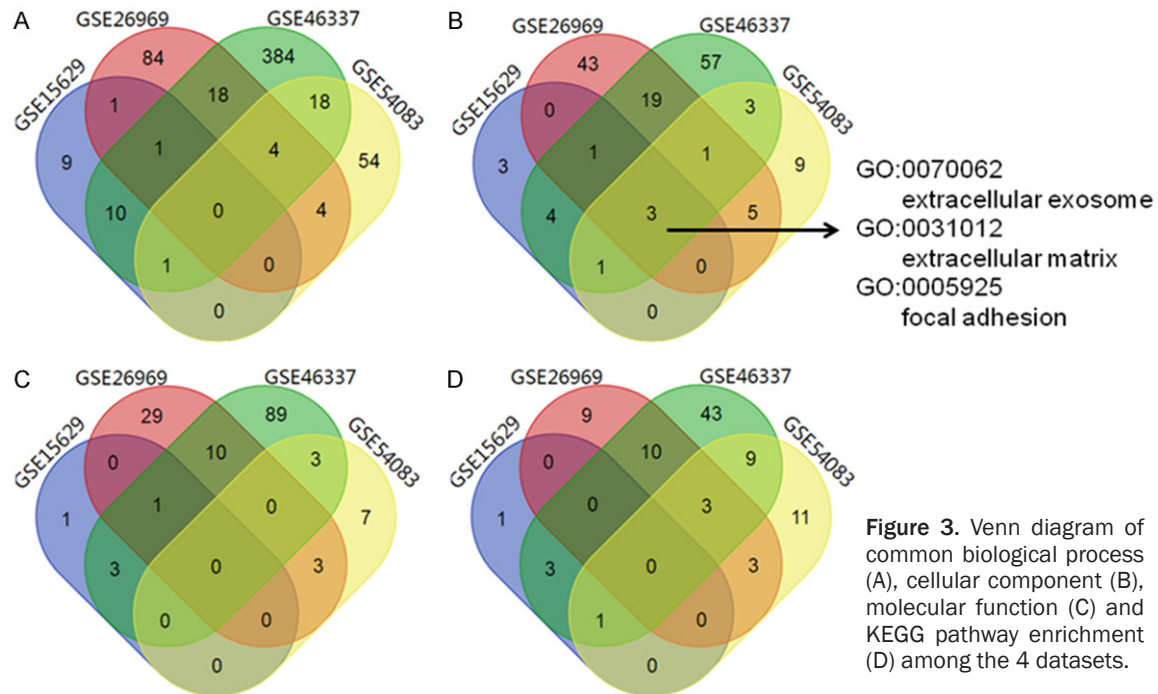


Figure 3. Venn diagram of common biological process (A), cellular component (B), molecular function (C) and KEGG pathway enrichment (D) among the 4 datasets.

Common GO function and KEGG pathway enrichment among the GEO datasets

As GO function and KEGG pathway enrichment analysis would facilitate an in-depth understanding of selected DEGs, the DAVID bioinformatic database was applied in this section. Because the results of GSE6551 showed little information for the GO function and KEGG analysis, probably due to the inadequate DEG numbers, the other DEGs of the other 4 datasets were imported into DAVID software. Significant GO functions ($P < 0.05$), including BP, MF and CC, as well as KEGG pathway enrichments were analyzed. Similarly, we compared whether there were common GO functions and KEGG pathway enrichments. We did not observe common BP, MF and KEGG pathways among the 4 GEO datasets (**Figure 3A**, **3C** and **3D**, respectively). However, three CCs were found to be common among the 4 datasets: extracellular exosomes, extracellular matrix and focal adhesion (**Figure 3B**).

Common DEGs in the Chinese population

As the ethnic heterogeneity for DEG cohorts from different GEO datasets, we investigated whether there were common DEGs between GSE46337 and GSE26969, which were Chinese population-based datasets. We found that

a total of 102 common DEGs were contained in the results of both datasets (**Figure 4A**).

PPI network analysis, GO function and KEGG pathway enrichment of common DEGs in the Chinese population

To depict the panorama of common DEGs from the two Chinese population-based datasets, we first made a PPI network of all common DEGs based on the information obtained from a string protein query in public databases (**Figure 4B**). The top 10 significant BP, MF and CC findings of the corresponding GO analysis (**Table 1**) and the top 10 significant KEGG pathway enrichments (**Table 2**) were listed.

Module screening from the PPI network

To discover key PPI networks and pathways involved in the pathogenesis of IA, the MCODE plug-in was used. Two modules were selected. In module 1, the enriched genes were involved with the major histocompatibility complex (MHC) gene cluster. The KEGG of module 1 generally showed that IA was mainly correlated with antigen processing/presentation, graft-versus-host disease, cell adhesion molecules, autoimmune diseases and infections (**Figure 5A** and **Table 3**). Additionally, KEGG enrichment analysis of the selected genes in module 2

Bioinformatic analysis of IA

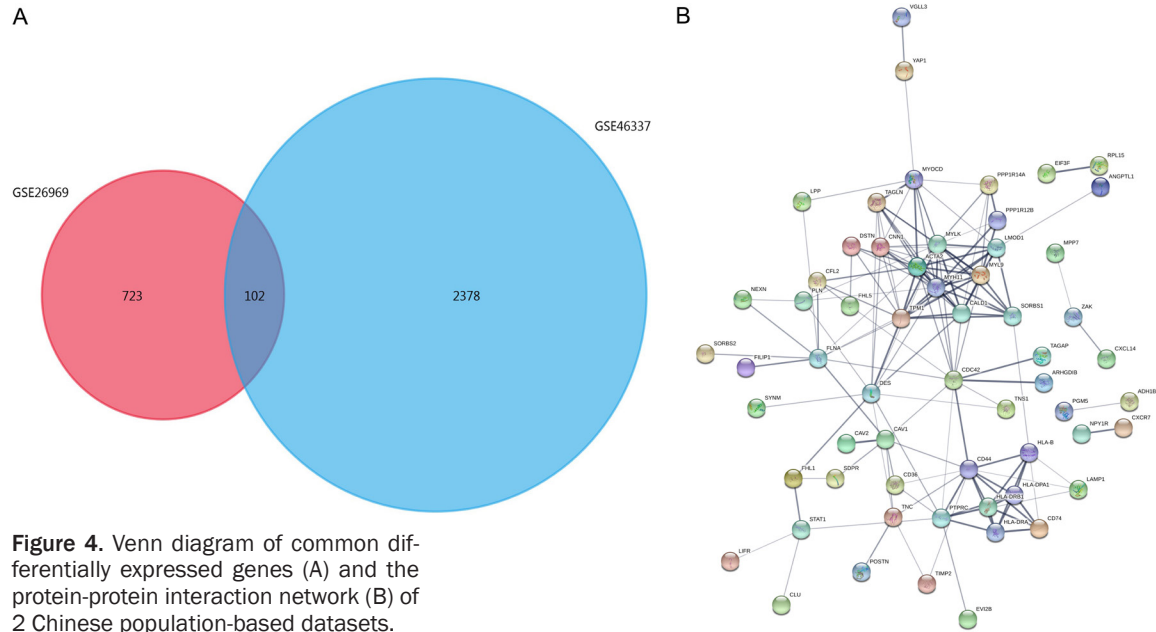


Figure 4. Venn diagram of common differentially expressed genes (A) and the protein-protein interaction network (B) of 2 Chinese population-based datasets.

revealed that IA had a significant correlation with vascular smooth muscle contraction (**Figure 5B** and **Table 4**).

Expression of TPM1 and TAGLN

The results (**Figure 6A** and **6B**) of qPCR showed that the expression of TAGLN in the unruptured IA vessels was significantly decreased in comparison with the normal superficial temporal arteries ($P = 0.003$), while there were no differences in TPM1 expression between the two groups ($P = 0.617$).

Discussion

Although the morbidity of stroke has declined in recent decades due to the improvements in detection technology and effective treatment of hypertension, the incidence of SAH, of which the ruptured IA is the predominant cause, do not show any trend of reduction, with approximately 23% of the survivors suffering from a significant restriction of lifestyle, ranging from a requirement for daily help up to full dependency [12]. Although evidence indicates that most IAs do not rupture, we can not distinguish the unruptured IAs from those that would eventually rupture. Therefore, investigating the molecule-based rupture risks of IA is urgently needed.

In previous studies, numerous mechanisms and biomolecules have been reported. Many

factors that influenced the stability of the dilated vessel wall might contribute to the rupture of IA, including degradation and disorganization of the extracellular matrix (ECM), formation of atherosclerotic plaques, decrease of reticular fibers and inflammation processes [13-16]. In the past decade, a large number of defining novel biomolecules, which might be potentially therapeutic targets for IA through high-throughput technologies, have been discovered. In this study, we conducted data mining from 5 gene expression datasets concerning common RNA in GEO databases. Interestingly, although numerous DEGs were detected from the 5 datasets, the results were notably heterogenic. No common DEGs were found. Moreover, there were also no common BPs, MFs and KEGG pathway enrichments among the 5 datasets. The results indicated that the pathogenesis of IA might be contributed by different genes or even biological functions in different populations. Krischek and colleagues presented a genetic association study for IA in different populations and found that variations in or near the JDP2 gene might be correlated with susceptibility in the East Asia population, rather than in the Dutch population [17]. We hypothesized that ethnicity-based differences might exist in the pathogenesis of IA among populations. Meanwhile, we might acknowledge that the influence factors of sample size and platform differences among studies should be also considered.

Bioinformatic analysis of IA

Table 1. Gene ontology analysis of differentially expressed genes associated with IA in Chinese population

Category	Term	Gene Count	%	P value	FDR (False Discovery Rate)
BP	GO:0006936~muscle contraction	9	8.8	1.7E-7	2.7E-4
BP	GO:0060333~interferon-gamma-mediated signaling pathway	6	5.9	5.3E-5	8.3E-2
BP	GO:0019882~antigen processing and presentation	5	4.9	2.7E-4	4.3E-1
BP	GO:0007155~cell adhesion	11	10.8	2.9E-4	4.5E-1
BP	GO:0031295~T cell costimulation	5	4.9	1.0E-3	1.6E0
BP	GO:0008015~blood circulation	4	3.9	2.2E-3	3.3E0
BP	GO:0006937~regulation of muscle contraction	3	2.9	2.8E-3	4.3E0
BP	GO:0001570~vasculogenesis	4	3.9	4.0E-3	6.1E0
BP	GO:0002504~antigen processing and presentation of peptide or polysaccharide antigen via MHC class II	3	2.9	4.2E-3	6.3E0
BP	GO:0007015~actin filament organization	4	3.9	8.1E-3	1.2E1
CC	GO:0005925~focal adhesion	19	18.6	3.2E-12	4.0E-9
CC	GO:0030018~Z disc	9	8.8	2.5E-7	3.1E-4
CC	GO:0009986~cell surface	15	14.7	1.3E-6	1.7E-3
CC	GO:0071556~integral component of luminal side of endoplasmic reticulum membrane	5	4.9	1.8E-5	2.2E-2
CC	GO:0030666~endocytic vesicle membrane	6	5.9	2.9E-5	3.6E-2
CC	GO:0070062~extracellular exosome	31	30.4	1.4E-4	1.7E-1
CC	GO:0012507~ER to Golgi transport vesicle membrane	5	4.9	1.8E-4	2.2E-1
CC	GO:0015629~actin cytoskeleton	8	7.8	1.9E-4	2.3E-1
CC	GO:0001725~stress fiber	5	4.9	2.1E-4	2.6E-1
CC	GO:0042613~MHC class II protein complex	4	3.9	2.2E-4	2.7E-1
MF	GO:0008307~structural constituent of muscle	6	5.9	3.0E-6	3.8E-3
MF	GO:0003779~actin binding	10	9.8	1.9E-5	2.4E-2
MF	GO:0042605~peptide antigen binding	4	3.9	4.5E-4	5.8E-1
MF	GO:0005515~protein binding	64	62.7	6.2E-4	8.0E-1
MF	GO:0051015~actin filament binding	6	5.9	7.4E-4	9.4E-1
MF	GO:0032395~MHC class II receptor activity	3	2.9	2.9E-3	3.6E0
MF	GO:0023026~MHC class II protein complex binding	3	2.9	3.3E-3	4.1E0
MF	GO:0004896~cytokine receptor activity	3	2.9	1.6E-2	1.9E1
MF	GO:0032947~protein complex scaffold	3	2.9	2.0E-2	2.2E1
MF	GO:0048365~Rac GTPase binding	3	2.9	2.0E-2	2.2E1

We listed top 10 significant terms in BP (biological process), CC (cellular component), and MF (molecular function) according to the *P* value, respectively.

Then, further analysis was conducted between two Chinese population-based datasets, aiming at discovering probable common genes and detailed pathogenesis in the Chinese population. Finally, we found that a total of 102 common DEGs between the GSE26969 dataset and the GSE46337 dataset. To achieve a more in-depth understanding of these DEGs, we performed GO function and KEGG pathway enrichment analyses of these DEGs. After analysis of two selected important modules for the common DEGs of the Chinese population in IA, we found that the enriched genes of IA were significantly associated with the MHC gene cluster and the vascular muscle contraction-related

genes. These two pathogenic candidates were not involved in the other analytic results obtained from the 3 GEO datasets.

MHC, also termed human leukocyte antigen (HLA), is a highly complicated hereditary system with highly polymorphic characteristics in humans. MHC plays highly important roles in immunity with the properties of antigen processing and presentation, as well as inflammation processes [18]. As early as 1847, Virchow hypothesized that IA formation was caused by inflammation [19]. There have been numerous studies concerning the relationship between MHC gene cluster-mediated inflammation and

Bioinformatic analysis of IA

Table 2. KEGG pathway enrichment analysis of differentially expressed genes associated with intracranial aneurysm in Chinese population

Term	Gene Count	%	P value	FDR (False Discovery Rate)	Gene List
hsa 04270: Vascular smooth muscle contraction	7	6.9	1.2E-4	1.4E-1	ACTA2, PPP1R12B, MYLK, CALD1, PPP1R14A, AVPR1A, MYL9
hsa 04510: Focal adhesion	8	7.8	3.8E-4	4.3E-1	PPP1R12B, MYLK, FLNA, TNC, CAV2, CAV1, MYL9, CDC42
hsa 04145: Phagosome	7	6.9	4.8E-4	5.4E-1	HLA-DPA1, LAMP1, ATP6VOD2, HLA-B, HLA-DRB1, HLA, HLA-DRA, CD36
hsa 05416: Viral myocarditis	5	4.9	5.2E-4	5.9E-1	HLA-DPA1, HLA-B, CAV1, HLA-DRB1, HLA-DRA
hsa 05152: Tuberculosis	7	6.9	1.0E-3	1.2E0	HLA-DPA1, STAT1, LAMP1, ATP6VOD2, CD74, HLA-DRB1, HLA-DRA
hsa 05332: Graft-versus-host disease	4	3.9	1.3E-3	1.5E0	HLA-DPA1, HLA-B, HLA-DRB1, HLA-DRA
hsa 04612: Antigen processing and presentation	5	4.9	1.6E-3	1.7E0	HLA-DPA1, HLA-B, CD74, HLA-DRB1, HLA-DRA
hsa 05330: Allograft rejection	4	3.9	1.8E-3	2.1E0	HLA-DPA1, HLA-B, HLA-DRB1, HLA-DRA
hsa 04514: Cell adhesion molecules (CAMs)	6	5.9	2.4E-3	2.7E0	HLA-DPA1, NEGR1, HLA-B, PTPRC, HLA-DRB1, HLA-DRA
hsa 04940: Type I diabetes mellitus	4	3.9	2.6E-3	3.0E0	HLA-DPA1, HLA-B, HLA-DRB1, HLA-DRA

We listed top 10 significant enriched pathways for the 102 common genes.

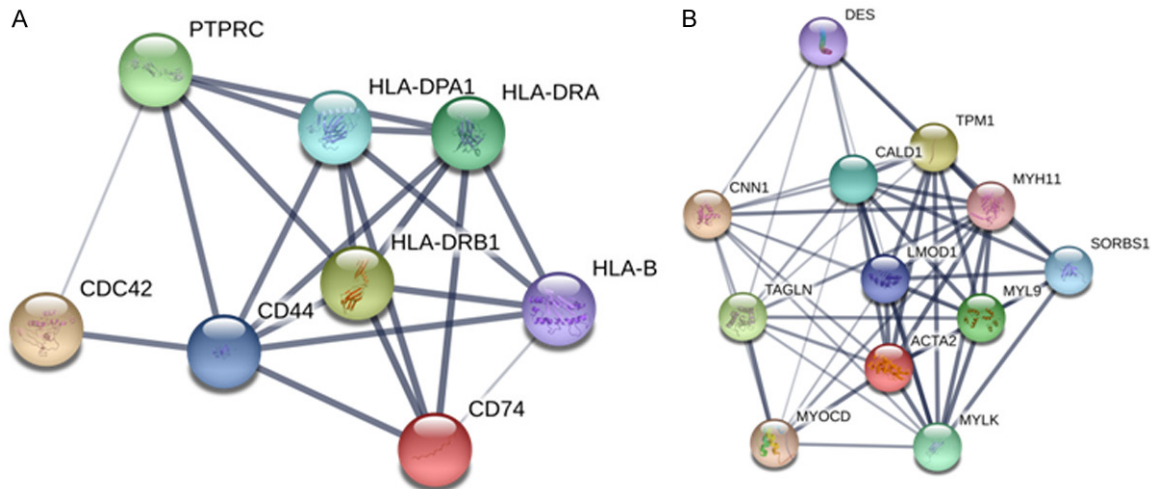


Figure 5. Two modules from the protein-protein network. (A) module 1 and (B) module 2.

IA formation [20-22]. An early study found that the expression of MHC II antigens in vascular smooth muscle cells (SMCs) might induce an attack of SMCs by specific T lymphocytes recognizing the SMCs as the autoantigens in the pathogenesis of vasculitis [23]. The immunohistochemistry data of IA tissues revealed the prominent infiltration of macrophages, which were the primary antigen presentation cell (APC) to express MHC II molecules. Krischek et al. performed a microarray-based analysis in IA patients and found a strong evidence of MHC class II gene over-expressions in human IA tissues in Japanese population [24]. Some clinical studies found that neurological outcomes of SAH patients resulting from ruptured IA might

be determined by the HLA phenotypes. Lye et al. found that the HLA-B7 phenotype in IA patients indicated a poor outcome, while HLA-DR3 might play a protective role in IA patients [25]. However, we found fewer in-depth mechanism investigations of MHC-related molecules on IA, most likely due to the complexity of the MHC gene cluster. As the heterogeneity of the HLA cluster, we did not test the expression of HLA-related genes between the unruptured vessels of IA patients and the normal superficial arteries.

To consider another aspect, it has been widely accepted that phenotypic modulation and dysfunction of vascular SMCs play highly important

Bioinformatic analysis of IA

Table 3. The enriched pathways of module 1

Term	Gene Count	%	P value	FDR
Antigen processing and presentation	5	62.5	4.60E-07	4.50E-04
Graft-versus-host disease	4	50	3.40E-06	3.30E-03
Allograft rejection	4	50	4.90E-06	4.70E-03
Cell adhesion molecules (CAMs)	5	62.5	5.70E-06	5.50E-03
Type I diabetes mellitus	4	50	7.20E-06	7.00E-03
Autoimmune thyroid disease	4	50	1.40E-05	1.30E-02
Herpes simplex infection	5	62.5	1.60E-05	1.50E-02
Viral myocarditis	4	50	1.80E-05	1.80E-02
Phagosome	4	50	3.50E-04	3.40E-01
Asthma	3	37.5	3.80E-04	3.60E-01
Tuberculosis	4	50	5.40E-04	5.20E-01
Intestinal immune network for IgA production	3	37.5	9.30E-04	9.00E-01
Staphylococcus aureus infection	3	37.5	1.20E-03	1.20E+00
HTLV-I infection	4	50	1.60E-03	1.50E+00
Inflammatory bowel disease (IBD)	3	37.5	1.70E-03	1.70E+00
Leishmaniasis	3	37.5	2.10E-03	2.00E+00
Hematopoietic cell lineage	3	37.5	3.00E-03	2.90E+00
Rheumatoid arthritis	3	37.5	3.20E-03	3.10E+00
Toxoplasmosis	3	37.5	5.70E-03	5.40E+00
Systemic lupus erythematosus	3	37.5	7.40E-03	6.90E+00
Influenza A	3	37.5	1.20E-02	1.10E+01

We listed top 10 significant enriched pathways. The enriched genes in module 1 were mainly involved with the major histocompatibility complex (MHC) gene cluster.

Table 4. The enriched pathway of module 2

Term	Gene Count	%	P value	FDR
Vascular smooth muscle contraction	4	33.3	1.70E-04	1.20E-01

The enriched genes in module 2 were significantly correlated with vascular smooth muscle contraction.

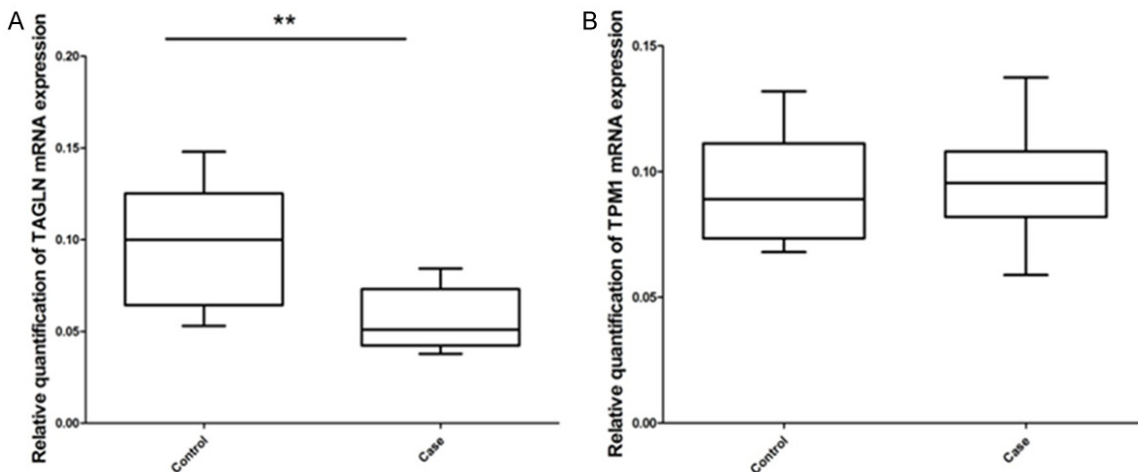


Figure 6. The expression levels of TAGLN and TPM1 mRNA from unruptured vessels of IA patients and normal superficial temporal arteries. A. Expression of TAGLN mRNA is decreased in unruptured vessels than controls ($P = 0.003$). B. No differences of the expression of TPM1 mRNA between the two groups ($P = 0.617$).

roles in the formation, progression and rupture of IA [26]. In the normal state, SMCs participate in contraction, regulation of blood flow and maintenance of blood pressure [27]. However, vascular SMCs exhibit a remarkable degree of plasticity when stimuli are exerted, such as inflammation and injury, transitioning from a quiescent contractile state into a proliferative synthetic state [28]. This effect leads to the dedifferentiation, progressively increasing the size that is mediated by the apposition of new layers of intramural thrombi within the vessel wall and consequently accelerates IA initiation [29]. In our study, module analysis revealed that IA was significantly associated with vascular SMC contraction, in which 12 hub genes were contained, including *DES*, *CMN1*, *CALD1*, *TPM1*, *TAGLN*, *LMOD1*, *MYH11*, *MYOCD*, *ACTA2*, *MYL9*, *SORBS1* and *MYLK*. We tested the expressions of *TAGLN* and *TPM1* in both the unruptured vessels of IA patients and the normal superficial temporal arteries because *TAGLN* and *TPM1* have not been replicated in IA-related studies. The results showed that *TAGLN* expression was decreased in the unruptured vessels. *TAGLN*, which was mainly expressed in vascular and visceral smooth muscle, participates in calcium-independent smooth muscle contraction. The vascular SMCs of *TAGLN*-deficient mice exhibited alterations in the distribution of the actin filament and the changes in cytoskeletal organization [30]. There have been inconsistent findings for *TAGLN* expression in aortic aneurysm tissues. Birós et al. found no differences between the abdominal aortic aneurysms and the control biopsies [31], while Ailawadi et al. found that human aneurysms expressed less *TAGLN* [32]. However, to the best of our knowledge, there have been no investigations of the association of *TAGLN* expression with IA.

Interestingly, we found that increased expressions and decreased expressions of DEGs were analyzed in some previous studies [11, 33, 34]. However, we did not undertake this analysis method in our study. DEGs that had significant associations with IA might have complex interactions and networks with each other, and the dysregulations of all DEGs should be integrally considered for the pathogenesis of IA. Therefore, we hypothesized that the combined analysis of all DEGs might be useful in profiling the pathogenic molecular network for IA and other diseases.

Some limitations for the study should be stated. First, we conducted the integral analysis by combining multiple established omic-based datasets, but we found that limited sample sizes were contained in each respective experiment. This might lead to the bias in statistical power and furthermore caused some false-positive and false-negative results. As for this bias, augmented sample sizes should be further conducted. Second, there might be some differences in molecular model or even pathogenic process in different subtypes of IA, which could be defined by sizes, locations and hemodynamic characteristics [35]. We did not distinguish the subtypes of IA from the primary studies. So we should be careful about the heterogeneity of pathogenic molecules among the different types of IA.

In conclusion, a total of 102 common Chinese population-specific DEGs were found between two Chinese population-based studies, and the MHC gene cluster and smooth muscle contraction-related genes might be of considerable importance in the pathogenesis of IA. Furthermore, the differential expression of *TAGLN* was initially confirmed and found to be decreased in the unruptured vessels of IA patients of Chinese population.

Acknowledgements

This work was partly supported by the Natural Science Foundation of Anhui Province [grant number: 1708085MH211].

Disclosure of conflict of interest

None.

Address correspondence to: Hongwei Cheng, Department of Neurosurgery, First Affiliated Hospital of Anhui Medical University, Jixi 218, Hefei 230022, P. R. China. Tel: +86-551-6292-2114; Fax: +86-551-6363-3742; E-mail: hongwei.cheng@ahmu.edu.cn

References

- [1] Malhotra A, Wu X, Forman HP, Grossetta Nardini HK, Matouk CC, Gandhi D, Moore C and Sanelli P. Growth and rupture risk of small unruptured intracranial aneurysms: a systematic review. *Ann Intern Med* 2017; 167: 26-33.
- [2] Nakaoka H, Tajima A, Yoneyama T, Hosomichi K, Kasuya H, Mizutani T and Inoue I. Gene expression profiling reveals distinct molecular

- signatures associated with the rupture of intracranial aneurysm. *Stroke* 2014; 45: 2239-2245.
- [3] Lawton MT and Vates GE. Subarachnoid hemorrhage. *N Engl J Med* 2017; 377: 257-266.
- [4] Sundstrom J, Soderholm M, Soderberg S, Alfredsson L, Andersson M, Bellocco R, Bjorck M, Broberg P, Eriksson M, Eriksson M, Forsberg B, Fransson EI, Giedraitis V, Theorell-Hagglow J, Hallqvist J, Hansson PO, Heller S, Hakansson N, Ingelsson M, Janson C, Jarvholm B, Khalili P, Knutsson A, Lager A, Lagerros YT, Larsson SC, Leander K, Leppert J, Lind L, Lindberg E, Magnusson C, Magnusson PKE, Malfert M, Michaelsson K, Nilsson P, Olsson H, Pedersen NL, Pennlert J, Rosenblad A, Rosengren A, Toren K, Wanhainen A, Wolk A, Engstrom G, Svennblad B and Wiberg B. Risk factors for subarachnoid haemorrhage: a nationwide cohort of 950 000 adults. *Int J Epidemiol* 2019; 48: 2018-2025.
- [5] Kan I, Ishibashi T, Sakuta K, Fujimura S, Yuki I, Kaku S, Kodama T, Kato N, Nishimura K, Aoki K, Sasaki Y, Karagiozov K and Murayama Y. Preoperative light transmission aggregometry values predict for thromboembolic complications after stent-assisted coil embolization. *World Neurosurg* 2020; 134: e731-e738.
- [6] Li M, Dong X, Chen S, Wang W, Yang C, Li B, Liang D, Yang W, Liu X and Yang X. Genetic polymorphisms and transcription profiles associated with intracranial aneurysm: a key role for NOTCH3. *Aging (Albany NY)* 2019; 11: 5173-5191.
- [7] Korostynski M, Piechota M, Morga R, Hoinkis D, Golda S, Zygmunt M, Dziedzic T, Moskala M, Slowik A and Pera J. Systemic response to rupture of intracranial aneurysms involves expression of specific gene isoforms. *J Transl Med* 2019; 17: 141.
- [8] Li L, Yang X, Jiang F, Dusting GJ and Wu Z. Transcriptome-wide characterization of gene expression associated with unruptured intracranial aneurysms. *Eur Neurol* 2009; 62: 330-337.
- [9] Pera J, Korostynski M, Krzyszkowski T, Czopek J, Slowik A, Dziedzic T, Piechota M, Stachura K, Moskala M, Przewlocki R and Szczudlik A. Gene expression profiles in human ruptured and unruptured intracranial aneurysms: what is the role of inflammation? *Stroke* 2010; 41: 224-231.
- [10] Rui YN, Xu Z, Fang X, Menezes MR, Balzeau J, Niu A, Hagan JP and Kim DH. The intracranial aneurysm gene THSD1 connects endosome dynamics to nascent focal adhesion assembly. *Cell Physiol Biochem* 2017; 43: 2200-2211.
- [11] Bo L, Wei B, Wang Z, Li C, Gao Z and Miao Z. Bioinformatic analysis of gene expression profile of intracranial aneurysm. *Mol Med Rep* 2018; 17: 3473-3480.
- [12] Molyneux A, Kerr R, Stratton I, Sandercock P, Clarke M, Shrimpton J and Holman R; International Subarachnoid Aneurysm Trial Collaborative Group. International Subarachnoid Aneurysm Trial (ISAT) of neurosurgical clipping versus endovascular coiling in 2143 patients with ruptured intracranial aneurysms: a randomised trial. *Lancet* 2002; 360: 1267-1274.
- [13] Chen L, Fan Y and Wan J. Screening of key genes of unruptured intracranial aneurysms by using DNA microarray data analysis techniques. *Genet Mol Res* 2014; 13: 758-767.
- [14] Rojas HA, Fernandes KSDS, Ottone MR, Magalhaes KCSF, Albuquerque LAF, Pereira JLB, Vieira-Junior G, Sousa-Filho JL, Costa BS, Sandrim VC, Dellaretti M and Simoes RT. Levels of MMP-9 in patients with intracranial aneurysm: relation with risk factors, size and clinical presentation. *Clin Biochem* 2018; 55: 63-68.
- [15] Lai XL, Deng ZF, Zhu XG and Chen ZH. Apc gene suppresses intracranial aneurysm formation and rupture through inhibiting the NF-kappaB signaling pathway mediated inflammatory response. *Biosci Rep* 2019; 39.
- [16] Signorelli F, Sela S, Gesualdo L, Chevrel S, Tollet F, Pailler-Mattei C, Tacconi L, Turjman F, Vacca A and Schul DB. Hemodynamic stress, inflammation, and intracranial aneurysm development and rupture: a systematic review. *World Neurosurg* 2018; 115: 234-244.
- [17] Krischek B, Tajima A, Akagawa H, Narita A, Ruigrok Y, Rinkel G, Wijmenga C, Feigl GC, Kim CJ, Hori T, Tatagiba M, Kasuya H and Inoue I. Association of the Jun dimerization protein 2 gene with intracranial aneurysms in Japanese and Korean cohorts as compared to a Dutch cohort. *Neuroscience* 2010; 169: 339-343.
- [18] Townsend A. Antigen processing. A new presentation pathway? *Nature* 1992; 356: 386-387.
- [19] Virchow V. Uber die akute entzündung der arterien virchows arch a pathol. *Anat Histopathol* 1847; 1: 272-378.
- [20] Ollikainen E, Tulamo R, Kaitainen S, Honkanen P, Lehti S, Liimatainen T, Hernesniemi J, Niemela M, Kovanen PT and Frosen J. Macrophage infiltration in the saccular intracranial aneurysm wall as a response to locally lysed erythrocytes that promote degeneration. *J Neuropathol Exp Neurol* 2018; 77: 890-903.
- [21] Hasan D, Chalouhi N, Jabbour P and Hashimoto T. Macrophage imbalance (M1 vs. M2) and upregulation of mast cells in wall of ruptured human cerebral aneurysms: preliminary results. *J Neuroinflammation* 2012; 9: 222.
- [22] Sakaguchi J, Takeshita M, Kagawa M, Izawa M and Takakura K. HLA-type of cerebral vasospasm patients after aneurysmal subarach-

- noid hemorrhage. *Neurosurg Rev* 1994; 17: 67-71.
- [23] Kosierkiewicz TA, Factor SM and Dickson DW. Immunocytochemical studies of atherosclerotic lesions of cerebral berry aneurysms. *J Neuropathol Exp Neurol* 1994; 53: 399-406.
- [24] Krischek B, Kasuya H, Tajima A, Akagawa H, Sasaki T, Yoneyama T, Ujiie H, Kubo O, Bonin M, Takakura K, Hori T and Inoue I. Network-based gene expression analysis of intracranial aneurysm tissue reveals role of antigen presenting cells. *Neuroscience* 2008; 154: 1398-1407.
- [25] Lye RH, Dyer PA, Sheldon S and Antoun N. Are HLA antigens implicated in the pathogenesis of non-haemorrhagic deterioration following aneurysmal subarachnoid haemorrhage. *J Neurol Neurosurg Psychiatry* 1989; 52: 1197-1199.
- [26] Fan W, Liu Y, Li C, Qu X, Zheng G, Zhang Q, Pan Z, Wang Y and Rong J. microRNA-331-3p maintains the contractile type of vascular smooth muscle cells by regulating TNF-alpha and CD14 in intracranial aneurysm. *Neuropharmacology* 2020; 164: 107858.
- [27] Stone OA, Carter JG, Lin PC, Paleolog E, Machado MJ and Bates DO. Differential regulation of blood flow-induced neovascularization and mural cell recruitment by vascular endothelial growth factor and angiopoietin signalling. *J Physiol* 2017; 595: 1575-1591.
- [28] Alexander MR and Owens GK. Epigenetic control of smooth muscle cell differentiation and phenotypic switching in vascular development and disease. *Annu Rev Physiol* 2012; 74: 13-40.
- [29] Korompoki E, Filippidis FT, Nielsen PB, Del Giudice A, Lip GYH, Kuramatsu JB, Huttner HB, Fang J, Schulman S, Marti-Fabregas J, Gathier CS, Viswanathan A, Biffi A, Poli D, Weimar C, Malzahn U, Heuschmann P and Veltkamp R. Long-term antithrombotic treatment in intracranial hemorrhage survivors with atrial fibrillation. *Neurology* 2017; 89: 687-696.
- [30] Elsafadi M, Manikandan M, Dawud RA, Alaje NM, Hamam R, Alfayez M, Kassem M, Aldahmash A and Mahmood A. Transgelin is a TGF-beta-inducible gene that regulates osteoblastic and adipogenic differentiation of human skeletal stem cells through actin cytoskeleton organization. *Cell Death Dis* 2016; 7: e2321.
- [31] Birois E, Walker PJ, Nataatmadja M, West M and Golledge J. Downregulation of transforming growth factor, beta receptor 2 and Notch signaling pathway in human abdominal aortic aneurysm. *Atherosclerosis* 2012; 221: 383-386.
- [32] Ailawadi G, Moehle CW, Pei H, Walton SP, Yang Z, Kron IL, Lau CL and Owens GK. Smooth muscle phenotypic modulation is an early event in aortic aneurysms. *J Thorac Cardiovasc Surg* 2009; 138: 1392-1399.
- [33] Wei L, Wang Q, Zhang Y, Yang C, Guan H, Chen Y and Sun Z. Identification of key genes, transcription factors and microRNAs involved in intracranial aneurysm. *Mol Med Rep* 2018; 17: 891-897.
- [34] Bo L, Wei B, Wang Z, Kong D, Gao Z and Miao Z. Screening of critical genes and microRNAs in blood samples of patients with ruptured intracranial aneurysms by bioinformatic analysis of gene expression data. *Med Sci Monit* 2017; 23: 4518-4525.
- [35] Signorelli F, Pailler-Mattei C, Gory B, Larquet P, Robinson P, Vargiolu R, Zahouani H, Labeyrie PE, Guyotat J, Pelissou-Guyotat I, Berthiller J and Turjman F. Biomechanical characterization of intracranial aneurysm wall: a multiscale study. *World Neurosurg* 2018; 119: e882-e889.

Bioinformatic analysis of IA

Supplementary Table 1. Information of five selected GEO datasets

No. of GEO dataset	Sample information	Ethnics	Target	Platform	Decision
GSE26969	3 IA samples vs. 3 normal superficial temporal arteries	China	Gene expression	Affymetrix Human Genome U133 Plus 2.0 Array	Included
GSE46337	2 IA samples vs. 2 middle meningeal arteries	China	Gene expression	Agilent-014850 Whole Human Genome Microarray 4x44K G4112F	Included
GSE54083	13 IA samples (including 8 ruptured IA and 5 unruptured IA) vs. 10 superficial temporal arteries	Japan	Gene expression	Agilent-014850 Whole Human Genome Microarray 4x44K G4112F	Included
GSE6551	2 IA samples vs. 3 intracranial arteries	American	Gene expression	Affymetrix Human Genome U133 Plus 2.0 Array	Included
GSE15629	11 IA samples (including 8 ruptured IA and 3 unruptured IA) vs. 5 full-thickness vessels of normal	Poland	Gene expression	Affymetrix Human Gene 1.0 ST Array	Included

Supplementary Table 2. Primers of real-time PCR

Gene	Accession No.	Forward Sequence	Reverse Sequence	Cat. No.
TAGLN	NM_003186	TCCAGGTCTGGCTGAAGAATGG	CTGCTCCATCTGCTTGAAGACC	HP229138
TPM1	NM_000366	GGCACCGAAGATGAACTGGACA	GCGTCTGTTCAGAGAAGCTACG	HP200346
GAPDH	NM_002046	GTCTCCTCTGACTTCAACAGCG	ACCACCCTGTTGCTGTAGCAA	HP205798